Journal of the Oceanographical Society of Japan
Vol. 37, pp. 9 to 20, 1981

Prediction of Ocean Waves Based on the Single-Parameter Growth Equation of Wind Waves (II)
Introduction of Grid Method*

Paimpillil S. JOSEPH**†, Sanshiro KAWAI** and Yoshiaki TOBA**

Abstract: The present study is a modification of the wave prediction model presented in the first paper of this title (KAWAI *et al.*, 1979) based on the Toba's (1978) single parameter equation of the wind wave growth. The introduction of a grid method reduces the two defects pointed out in KAWAI *et al.*, i.e., the absence of the prediction of certain instants at fixed points, and the concentration of wave energy at certain points in the wind direction, arising from the lack of treatment of the lateral spreading of wave energy around the wind direction. The new model is applied to the same set of data. The results shows overall improvements, such as the elimination of certain overestimate in the first study and the coincidence of the predicted maximum with the measured one. The swells are separately hindcasted and a very good agreement with measurement is obtained.

1. Introduction

In a recent paper, KAWAI *et al.* (1979), hereafter referred to as "I", discussed the merits and demerits of various wave prediction models and developed a new method based on the single parameter growth equation of wind waves by Toba (1978). At almost same as "I", GUNTHER *et al.* (1979) has published an extension of the JONSWAP studies of HASSELMANN *et al.* (1973, 1976). Both GÜNTHER *et al.* (1979) and "I" contain incidentally a section titled "background", and similar thoughts can be found between them, namely the recognition of the nonlinear processes as the overriding process in the dynamics of growing wind-waves, and the idea to parameterization of these processes eventually on an empirical bases. However, there are different features in the two models. As to nonlinear processes, GÜNTHER *et al.* (1979) stands on the theory of weakly nonlinear wave-wave interaction. On the other hand, we consider that the strongly nonlinear processes involving the local wind drift are important. The manifestation of these processes is conspicuous similarity of simple three-seconds power law and the σ^{-4}-type spectral form (TOBA, 1972, 1973 and 1978), and thus our prediction model pursues a single parameter, whereas GÜNTHER *et al.* (1979) five parameters which characterize JONSWAP-type spectra.

It is very interesting that MITSUYASU *et al.* (1980) have recently reported quasi-equivalence of the JONSWAP spectrum and Toba's spectrum at the high-frequency side. If the both spectral forms are essentially equivalent on empirical bases, our model has a merit of much simplicity.

In "I", a "wave packet following method" was employed, in which wave packets originate with zero initial energy and propagate in the local wind direction. At each time step, the position of the wave packet is determined, and the wind velocity at such point is interpolated from the winds at the nearby grids. For the next time step, the wave packet is allowed to develop and propagate in the new interpolated wind direction. This process is repeated for each wave packet with each time step, and the average of the height of the wave packets entering into a region defined around the prediction site is taken to represent the wave height for the site. Though, no spatial smoothing was applied to the wave energy on its way to the prediction site. This kind of the propagation may make the number of wave packets to get concentrated at certain zones at any in-

* Received Sept. 8, 1980 revised March 6 and accepted March 11, 1981.
** Geophysical Institute, Faculty of Science, Tohoku University, Sendai 980, Japan
† Present address: Physical Oceanography Division, National Institute of Oceanography, Goa 403004, India

stant of time, depending on the wind field. If the prediction site falls in a region of diverging winds, the number density of the wave packets entering into the region defined around the prediction site for the spatial averaging may sometimes reduce to zero, making a time series of the wave prediction at the site impractical. This is the first defect of the method in "I". Secondly, the wave energy is bound in the wind direction, developing and propagating along the local wind direction. This treatment may make the energy concentrated at certain points when the nonuniformity of the wind is great. But in reality, the wave energy is distributed around the local wind direction with an associated lateral spreading. These were the main shortcommings of "wave packet following method" in "I" and it was indicated that an allowance for proper coupling between the wave packets may sufficiently smooth out energy centralization tendency. In the present study, this point is overcome by allowing the interaction of different wave packets with the use of an interpolation method for the wave energy. As a result of the interpolation, the present method can also give a time series of the wave properties at any fixed point of the study region.

2. Numerical scheme of prediction

2.1. *Basic equation*

The basic equation used for the present study is exactly the same as in "I":

$$\frac{DE^{*2/3}}{Dt^*} = G_0R[1-\mathrm{erf}(bE^{*1/3})] \qquad (1)$$

where $E^* \equiv g^2E/u_*^4$ with E as the wave energy per unit area, $t^* \equiv gt/u_*$, a nondimensional time, g is the acceleration of gravity, u_* the friction velocity of air and $\mathrm{erf}(x)$ is an error function defined as,

$$\mathrm{erf}(x) \equiv 2/\sqrt{\pi}\int_0^x \exp(-\zeta^2)d\zeta \qquad (2)$$

The other quantities are nondimensional empirical constants:

$$G_0R = 2.4\times10^{-4}, \quad b = 0.12 \qquad (3)$$

The basic equation is a first order differential equation, which can be easily numerically integrated as shown in the appendix of "I" and this will give the wave energy at every time step. From the nondimensional energy, any other properties of the wave field can be obtained through the similarity relationships. The significant wave height H can be calculated by the equation of LONGUET-HIGGINS (1952) as,

$$E = H^2/16 \qquad (4)$$

Then the period T of the significant wave, is determined from the three-seconds power law, which was proposed by TOBA (1972) as representing the similarity in growing wind waves:

$$H^* = BT^{*3/2} \qquad (5)$$

where H^* and T^* are the nondimensional wave height and period defined as $H^* \equiv gH/u_*^2$ and $T^* \equiv gT/u_*$ respectively and B is a nondimensional empirical constant which takes a value of 0.062 for the case of significant wave.

2.2. *Initial and boundary conditions*

At the boundary coincident with a coast line (physical boundary), it is proper to take the energy density as zero for offshore winds. For onshore winds, it is assumed that a wave arriving at a coast is completely absorbed by the land. Hence, for onshore winds, a coastal grid point behaves as an inner one. For any numerical boundary which has to be fixed inside the sea, the problem of waves entering through such boundaries into the prediction region needs to be considered. The numerical boundaries are fixed at such a distance away from the selected point of wave prediction that even if a wave enters through such a boundary at any time during the prediction interval, the distance between the selected prediction point and the boundary is large enough for the wave at the boundary not to influence the prediction at the desired site during the prediction time interval. After fixing a numerical boundary as above, it is also reasonable to assume it to act in the same manner as that of the coast.

As for the initial condition, the wave energy is assumed to be nil everywhere. This assumption seems to be improper because some wave energy may be present in the ocean for all times. The error arising from this initial condition is considered to diminish at sufficiently later time steps. The time steps necessary for the effect of the initial conditions to be smoothed out and disappeared may be 3 to 4 days for large calculation domains.

2.3. Time wise integration and smoothing

Taking a system of equally spaced grids, we can determine the nondimensional energy at each grid at any time by integrating (1). The time step Δt is so fixed that the distance traveled in Δt with the possible largest group velocity should be less than one grid size. In the present study, (1) is integrated with the same iteration method discussed in "I". The position of the wave packet can be calculated from the group velocity of the wave packet which is estimated from the peak period by the linear wave theory. As the group velocity is changing with the development of waves, an average value for it for the interval Δt is used for fixing the position of the wave packet.

After fixing the new positions of the wave packets originated from all the grids, the wave energy exactly present at each grid has to be calculated through interpolation among the energy at the new positions, for allowing the coupling between various wave packets. A vector interpolation method is used here (more details in Appendix), which uses the energy at the new positions of three nearby grids to the particular grid at which the interpolation is going on and also its own energy at the new position and this is done at each time step. This interpolation may provide a smoothed energy at the grid, which represents a smoothed value for the region of one square grid size. Though, at a first glance, this systematic step by step interpolation seems to give excessive error due to oversmoothing, a test with a uniform wind showed the maximum difference between the nonsmoothed and few thousand times smoothed values of wave height to be lesser than 20% even at the points where the gradient of the wave height is maximum. Hence, it is taken that the present interpolation at each grid for each time step is not giving any serious defect to the prediction. For the cases of a numerical boundary, the energy interpolation is limited to the onshore winds as the boundary condition attributes zero energy to the boundary grids for an offshore wind. The wave height and period at each grid are then calculated from the interpolated new energy. For the next step, the interpolated wave energy and its direction at each grid is taken as the initial condition.

After one set of calculations for all grids is over, a check is made to see whether any of the wind wave energy is transferred to the swell, in accordance to the transfer condition discussed in later Section. If the transfer condition is satisfied, the swell has to be predicted separately as in Section 2.4.

2.4. Formation of swell and its propagation

For the spatially and temporally varying wind, the wave energy is assumed to adjust to the new wind direction in accordance with the following equation used in "I",

$$\frac{E_{\Delta\theta}}{E}=\cos^{k}\Delta\theta \qquad (6)$$

where k is taken as a variable with values from 0 to 4. This equation is suitable for slowly varying wind systems, excluding the lateral and the adverse winds. The adverse and the lateral winds are defined in the same manner as in "I".

It is assumed here that for the adverse winds, the preexisting wave vanishes in one time step and a new wind wave starts to develop from zero energy, along the new wind direction. For lateral winds the wind wave is assumed to change into the swell propagating in the old wind wave direction, and at the same time a new wind wave is assumed to develop from zero initial energy along the new wind direction.

In addition to the swell formation as above, swell can also form if a wind wave attains a fully developed state for a particular wind if a sufficient decrease in the wind speed changes the state of the underdeveloped wave into an overdeveloped state for the new wind. The latter case may be more frequent in the ocean. Here, some criterion is necessary to classify a given wave into a fully developed, overdeveloped or as an underdeveloped one. Here, we introduce the condition that the wind wave changes into swell for the nondimensional peak period greater than 248 (TOBA, 1978). If the wind speed decreases suddenly, the total energy is redistributed between the swell and the wind wave so that the wind wave is saturated for the new wind speed.

The prediction of the swells is made as in "I" with the use of the simple empirical relation proposed by BRETSCHNEIDER (1968).

In the present grid method, the actual fetch (the fetch over which the wind wave was developing up to its arrival at the particular grid)

needed in the swell prediction formula, is not readily available. For a wind wave which changes to swell at a certain instance due to a change in the wind direction or wind speed, the equivalent fetch required for the formation of that particular wind wave under the prevailing wind of the last time step at the point of swell formation may be regarded as the fetch for the present purpose. This can be calculated from the empirical relation of WILSON (1965), modified in the following way,

$$H^*=0.30[1-(1+0.004(C_DF^*)^{1/2})^{-2}]C_D^{-1} \quad (7)$$

where C_D is the drag coefficient of the sea surface and which is equivalent to the integration of the fetch limited form of the single parameter growth equation of wind waves (TOBA, 1978).

If the swell formation is by the energy saturation, (7) is not applicable for the determination of the minimum fetch, as the nondimensional height attains a constant value and becomes independent of fetch. For such cases, the nondimensional fetch ($F^*\equiv gF/u_*^2$) associated with the following saturated nondimensional wind wave energy,

$$E^*=3.7\times10^3 \quad (8)$$

and with the following value

$$F^*=1.3\times10^9 \quad (9)$$

as given in TOBA (1978) is used in the present study. As the minimum duration of the intense winds needed for a fully developed sea may generally be more than the total time of the prediction calculation, the formation of swells by the fully developed sea may be limited to the cases of light winds or associated with a decrease in the wind speed.

3. Hindcast examples

3.1. Small scale case

For a small scale test, the region near the Shirahama tower is selected as in "I". The wind at the tower is considered to represent the wind field of the entire fetch, since the waves reaching the tower were developed in the nearby regions as has established in "I". A time step of 5 minutes and square grids spaced at 500 m are taken. As the prediction

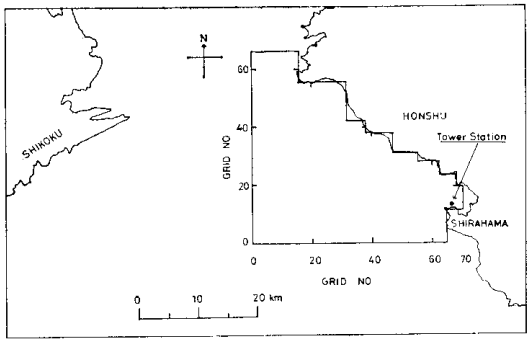

Fig. 1. Locality of the Shirahama Tower Station with the numerical boundaries and the grid system.

calculations were not started at an advance time with respect to the time of the first prediction at the site, the accuracy in the first few predictions is not good. As the wind field is temporally changing one, allowance for the directional shift between the wind and the wave directions is done as per the equation (6), testing it with different values of k and the results are given in Fig. 2.

From the hindcast results of Fig. 2, it seems that the present model's ability to reproduce the trends in the wave developments remains to be excellent, if the directional change is treated properly. Though the trends are well represented for most of the time, an overestimate of the waves during the end of the prediction duration is well noticeable. We will look at this point later. Now, we will look at the results for different values of k. Independent of k, the wave heights are attaining nearly same value during the prediction period, with the confinement of the large deviations associated with k to the times of great angular deviation in wind direction. The coincidence of the predictions for all values of k during the times of small deviations in wind direction (1430 to 1600 JST) and of marked differences associated with greater wind shifts (1145 to 1330 JST) indicate that if a prediction is not needed immediately after a time of considerable change in wind direction, any value of k from 2 to 4 is suitable to provide a good prediction. The value of k equal to 4 seems to have a best fit for the total period of prediction of this case.

As the overestimates during the last time steps are common for the results with the different values of k in equation (6), it is reason-

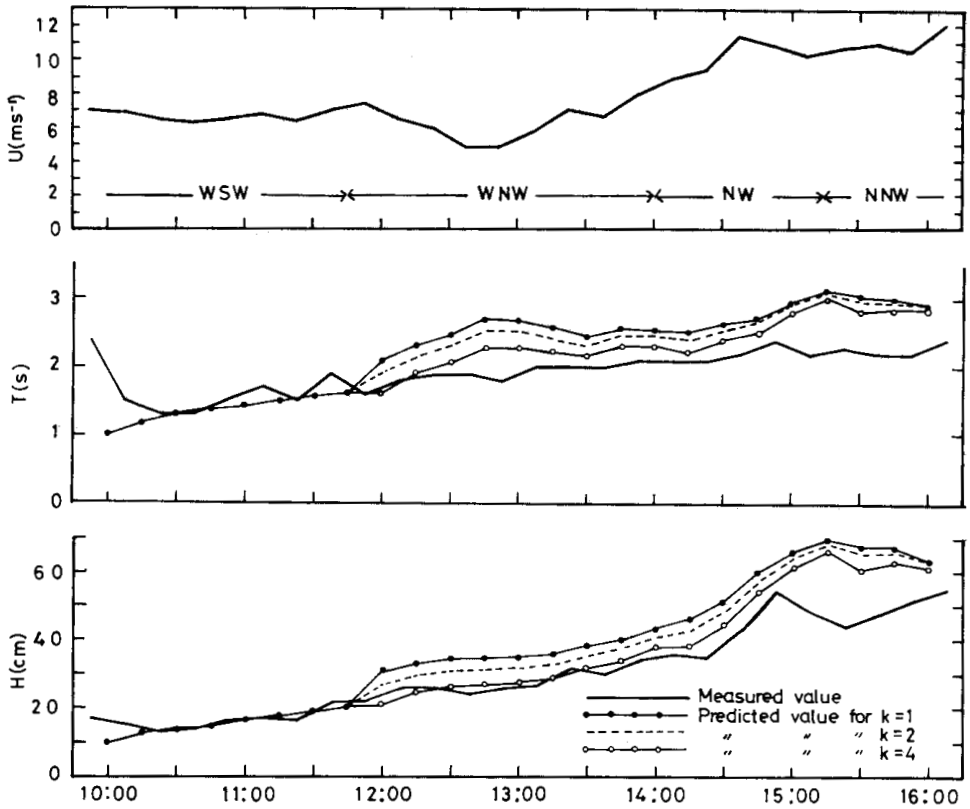

Fig. 2. A comparison of the time series of the predicted wind wave significant heights and the periods with its measurements at the Shirahama Tower Station on 10th Nov. 1969. The upper figure shows the time series of the winds measured at the tower.

able to assume that this overestimate may not be connected with the problem of energy adjustment to the new wind directions but may be related with the wind field as a whole, probably with a failure of the homogeneity assumption of the wind field for the entire region. From 1500 JST onwards the wind started blowing from the land and in the regions near to the coast the wind may not be as intense as at the tower site. This somewhat shadow region may considerably reduces the development of waves and this may be the reason for the much lower measured waves at the tower site. This overestimate was also seen in "I".

The predicted trend of the wave periods is also in good agreement with the measured trends, but having some overestimates for most of the prediction time.

3.2. Large scale case

Many wave prediction models have been tested for the waves caused by North Atlantic cyclones of December, 1959, whose wind and wave data were well documented by BRETSCHNEIDER *et al.* (1962). For comparison with other models, the present model is applied also to this situation, with the same data and grid as in "I". The waves measured by the ship "Weather Reporter" are compared with the hindcasted ones at a prediction site called J. But, it needs to be noticed here that the ship position deviated much from the J point during certain intervals of prediction time.

As mentioned in Section *2.2*, zero energy is taken as the initial condition. To examine the influence of this rather artificial condition, the wave on 16th December was calculated for three different initial times, 10th, 12th and 14th December, respectively. The predicted results for the first two cases are almost the same, indicating that, in this case, almost all the influence of the initial condition may vanish if the initial time is at least 96 hours in advance

of the time from which prediction is required.

The hindcasts are also performed with four different values of k (0 to 4) in equation (6), but no significant difference in results is found. Hence, only the results for $k=4$ are presented hereafter. The independence of the predictions of the large scale case on the value of k was discussed well in "I" and the arguments presented there seem to be quite satisfactory.

For the prediction of swells the following method is adopted instead of the interpolation method used for wind waves. The spatial average of the swells, except those with height less than 2 m, entering into the circle which has a radius of one grid and the J point as its center, is considered as the swell at the J point. This method was adopted because of the number of swells being few, the random distribution of these swells around the grid point and the possibility of many different directions of swell approach.

The measured properties of both the wind waves and the swells were calculated from the observed power spectra given in BRETSCHNEIDER *et al.* (1962). In the calculation, the following criterion was used for separating the swell and the wind waves,

$$C \geq 1.37\, U_{10} \qquad (10)$$

where U_{10} is the wind speed at 10 meter height and C is the phase velocity of the wave component determined from the linear theory. Observed spectral peaks are classified into swell and wind wave ones, according to (10). The equation (10) essentially corresponds to the criterion of (8). If (10) is satisfied, it is classified into swell. If the measured spectrum has plural peaks and they consist of different classes, the energy is separated at the frequency with the least energy between the two spectral peaks belonging to two different classes. The total energy of the waves with frequency lower than this is taken as of the swell regime and remaining as of the wind wave regime. If the wave spectrum is with a single peak either in the

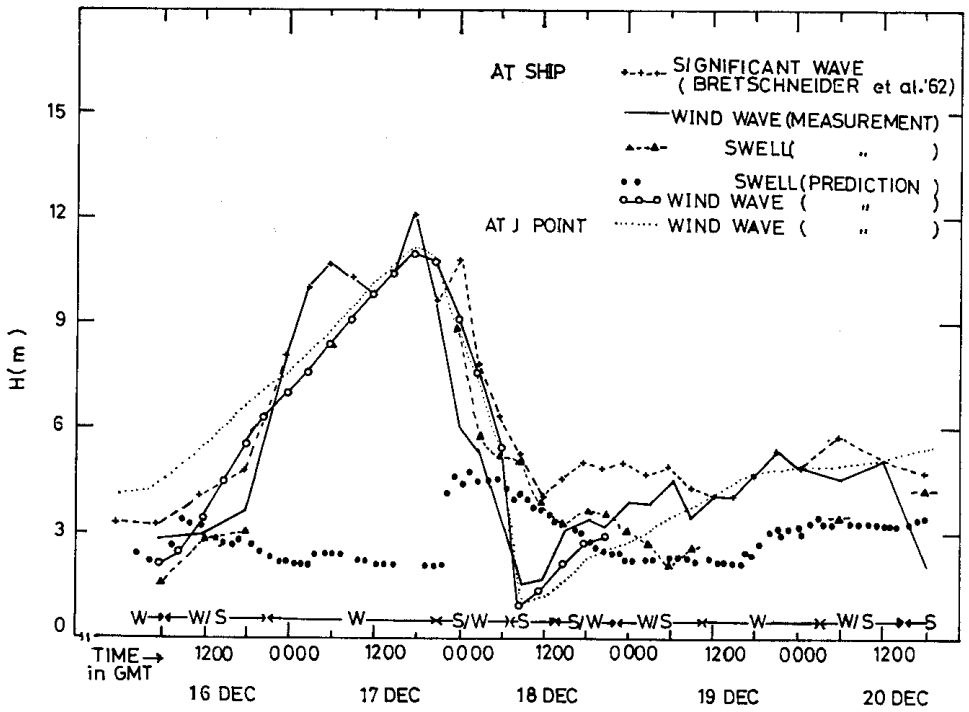

Fig. 3. A comparison of the predicted wind waves and swells of the point J and the ship position with their measured counterparts. The inserted letters have the following meaning. W: wind wave dominance; S: swell dominance; S/W: nearly equal wind wave and swell energy, with swell energy slightly in excess; W/S: nearly equal wind wave and swell energy, with wind wave energy slightly in excess.

wind wave or the swell domain, the entire energy of the spectrum is taken as of the wind waves or swell, depending on the position of the peak. If all the plural spectral peaks belong to a single class, the total energy of the wave field is given to that class. From the separated portions of the energy, the significant height for each class is calculated by (4). The period corresponding to the spectral peak in each portion is taken to represent its significant period.

The hindcasted wind waves and the swells at the J point are compared with those measured at the ship position, obtained in the above mentioned manner. The wind wave predictions at the exact ship positions are made available by linearly interpolating the wind waves for that point from the wind waves of nearby four grids. As the regicn defined around the J point for the swell prediction includes a considerable area including the ship position during most of the prediction time, no separate swell calculations for the ship locality are done. For the durations at which the ship positions are not given, it is taken that the ship was remaining at the J point. The comparison of wave heights is shown in Fig. 3.

During the initial stages of the prediction (on 16th December) the predicted waves at the J point showed considerably high values than the measurements. This disagreement is cleared by using the interpolated prediction values at the ship position for the comparison with the measured values, as seen in Fig. 3. In that interval on 16th December, the ship was on its way to the J point and was at most 1.5 grids away from the J point.

The predictions for the 12 hour period (0000 GMT to 1200 GMT) on 17th December showed much lower predicted wave heights than their measurements. As a probable reason for this, the accuracy of the wind data is suspected and a comparison of the measured winds at the ship position is made with the wind data used here for the prediction of the waves for the 12 hour duration (0000 GMT to 1200 GMT) on the above day. This comparison is shown in Fig. 4. It indicates that the interpolated winds are too smoothed and much lower than that of the real winds. As the present wave prediction depends on the local wind for the further development, the smoothed out lower winds for the

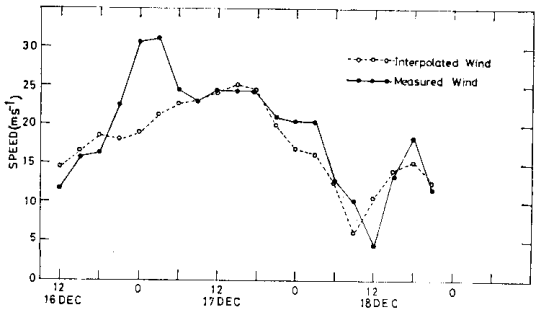

Fig. 4. A comparison of the measured wind speeds by the ship with the wind data used for prediction, for the duration of the greatest disagreement in wave prediction and measurement (for details see the text).

above periods are expected to give a similarly smoothed lower development for the wave field. ISOZAKI & UJI (1973) had suggested a similar explanation for the low hindcasts for the above period.

Another feature of the predicted waves is the presence of some energy in the swell domain during certain periods of wind wave dominance in the measurements. Such predicted swells are clearly seen from 2100 GMT on 16th to 2100 GMT on 17th and also again from 1030 GMT on 19th December to 0300 GMT on 20th December. Comming to the intervals of swell dominance in measurements (around 0000 GMT on 18th), the hindcasted wind waves seem to represent the trends of the swell with the height of the wind waves remaining to close to that of the swells. The predicted swells for the above periods remained at a very low level in comparison to their measured counterparts. The first feature is considered to be associated with the accuracy in the spectral measurements when any one of the two classes has very great energy concentration in it and also with the swell-wind wave transfer problem. The resemblance of the predicted wind waves with the measured swells may be due to the problem associated with the energy separation into different classes. These points will be looked in detail in the next section.

For comparing the results of the present model with that of the others, the significant height at J calculated from the total energy of the predicted wind waves and swells at the above point is used. This comparison is shown in

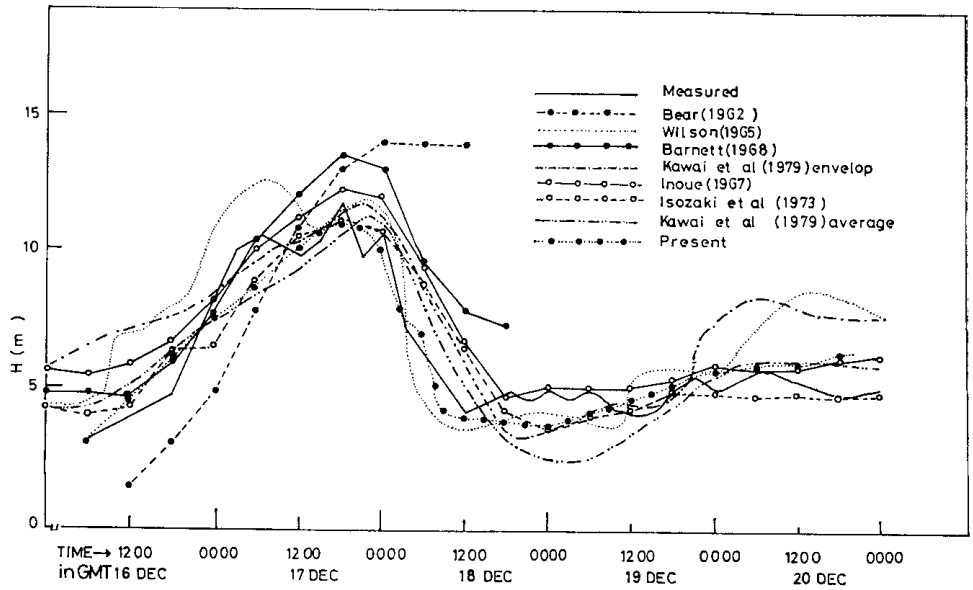

Fig. 5. Comparison of the significant wave height and the point J with that of the other model results.

Fig. 5. Most of the other models included in the figure correspond to the spectral wave prediction method except that of WILSON (1965) and of "I". The overestimates at the J point on 16th December seem as a common feature for all model results. The reason behind this overestimate remains to be the same as already mentioned. The noticeable underestimate in "I" (average value) for the periods from 1200 GMT on 18th to 1200 GMT on 19th December is considerably removed in the present case. This improvement has been achieved from the treatment of the wind wave energy at the instants of the swell formation. In "I", the wind wave energy is taken as zero for such instants, while in the present case it is given the saturated energy value possible at the new wind speed and this will give much more wind wave energy at the next step. The significant overestimates found only in WILSON (1965) and in "I" (envelop value) on the 20th December are absent in the present results. But, the predicted average values in "I" for the above period agree well with the measurements. This indicates that the taking of the envelop values, as also done in WILSON (1965), to represent the prediction results may be the reason behind this overestimate. Though the average values can be calculated in "I", it may take considerable amount of calculation. In the present case, the average values are always available at the grid and this is an advantage of the present model. Additionally, in "I" the attainment of the highest height was delayed much in comparison with the time of observation of the highest wave height. In the present model, the coincidence of both seems to be remarkable.

The measured peak periods corresponding to the wind waves and the swells at the ship position are compared with the hindcasted wind wave period and the average swell period, respectively. A comparison, Fig. 6, reveals that the hindcasted periods of the wind waves represent the trend well but its values are slightly lesser than that of the measurements. For the swell dominance duration, the average periods of the swell seems to be close to the measured period of the swells. The reason behind the presence of considerable swell periods during the absence of a peak in the swell regime and the lower values for periods on the first half of 17th December is the same as mentioned for the case of heights. As the wave period predictions are not available in the other models, a comparison is not possible.

4. Discussion

One of the reasons why predicted swells have

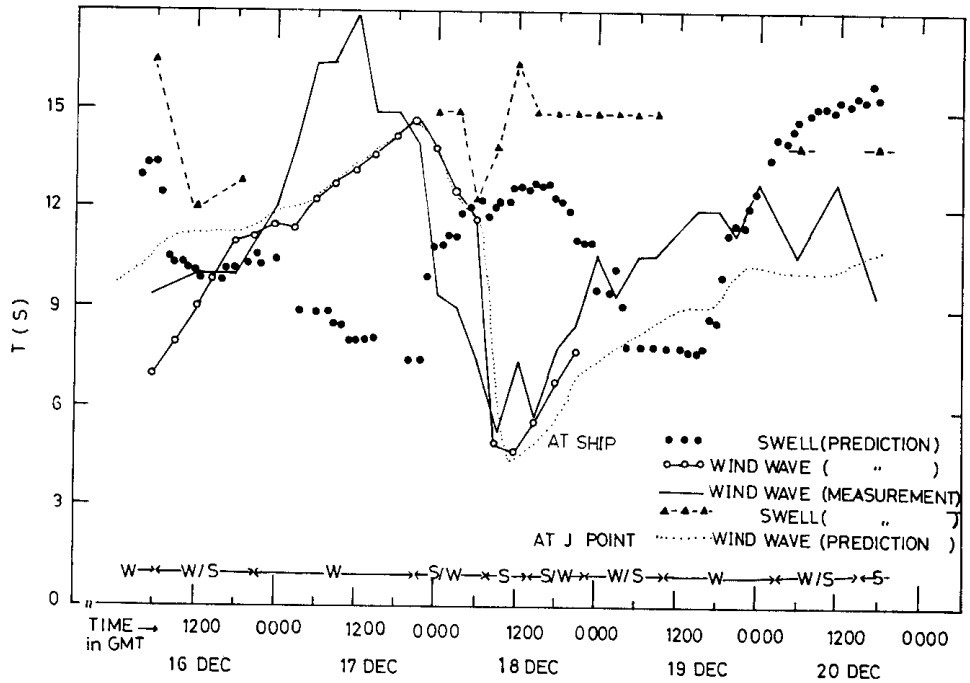

Fig. 6. A comparison of the wind wave peak period and the average swell period at the point J and the ship position with their measured counterparts. The meaning of the inserted letters remains the same as of Fig. 5.

considerable height at the instants of wind wave dominance may be associated with the observational problems. When the energy of wind wave differs from that of swells by 2 order or so, the practical estimation of the spectral density may lack in accuracy for less energetic part. Secondly, the empirical relation used for swell prediction neglects the influence of wind on the swell. Most of the predicted swell in the wind wave dominance intervals may be modified into the wind waves in accordance to the criteria of swell-wind wave transfer given by (10). In such a change, the swells will disappear, but the associated energy adjustments in the wind wave regime and the further growth of the wind waves with the modified energy need to be treated carefully. In the present study, this problem has not been treated at all. Here, it need to be mentioned that HATORI *et al.* (MS.) have shown that the growth of a regular wave (swell in the present context) entering into a wind field having greater speed than its phase speed depends on the steepness of the regular wave and on the ratio of its frequency to the peak frequency of wind waves that would occur in the absence of the regular wave. They showed that, four distinguishable stages are present in the evolution of a regular wave. At the first stage, wind waves appear as in the usual manner, but the regular wave remains unaffected at constant. In the second stage, the development of the wind waves is damped with an increase in the regular wave height, which is followed by the third stage in which regular wave rapidly grows by a direct energy gain from the wind and the wind waves attenuate. At the fourth stage, the regular wave itself breaks down to become irregular wind waves. This study suggests a strong interaction between the wind wave and regular wave at the second stage. These phenomena should be studied further and taken into account in the future prediction model.

Next, we have to look for the reasons why the predicted wind waves have as much energy as the measured swells for the periods around 0000 GMT on 18th December. This confusing fact may be associated with the swell-wind wave energy separation. When the frequency which separates the two regimes in accordance with

the phase velocity condition is very close to the frequency of the spectral peak, it may be difficult to decide whether the peak belongs to the swell or wind wave regime, since the energy separation in the real process is not as critical as in (10). On this point further study is needed.

Finally, for an estimate of the error in the predicted values with the measurements, we have used the r.m.s. value of the difference between the above two, which gives the following respective values of 1.24 m, 1.83 m and 1.25 m for the wind wave, swell and for the dominant wave. If the same format as used in ISOZAKI (1978) and in "I" is used, the mean of the above mentioned deviations along with their respective standard deviations give the following respective values of 0.06 ± 1.27, -0.58 ± 1.66 and 0.57 ± 1.10 for the wind wave, swell and for the dominant wave. Comparing with the error in "I", the error for the dominant case seems to be smaller in the present.

Acknowledgements

The authors express their deep thanks to Dr. I. ISOZAKI, Meteorological Research Institute, JMA, for his kindness to lend them the data of the Atlantic case. One of the authors (PSJ) wishes to express his thanks to the Japanese Ministry of Education, Science and Culture for the grant of a fellowship and to the National Institute of Oceanography, Goa, for granting him study leave for the period. This study was partially supported by the Grant-in-Aid for Scientific Research by the Ministry of Education, Science and Culture, Project No. 402503. This study was also performed as a member of the Commission of Development of Ocean-Wave Prediction Techniques, which was organized in the Japan Weather Association in August, 1978. The computations were done by the use of FACOM-230-38 of the Computer Center of Tohoku University.

Appendix

The iteration scheme used in the study is exactly the same as in "I" and the equations A1 to A11 in "I" are used here in the same order.

The distance covered by a wave in one time step Δt along the x and y directions is calculated rom the distance ΔF along the wave direction by

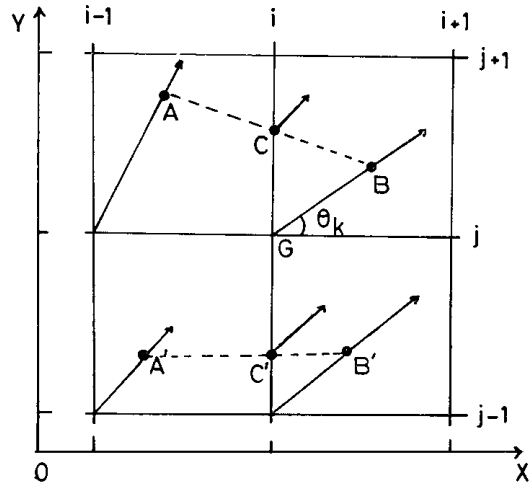

Fig. 7. Schematic diagram showing the energy interpolation for a selected grid G. The A, A′, B, B′ represent the new positions of 4 wave packets started from their respective grids, after their propagation shown by arrows for unit time step. The C and C′ represent new positions of wave energy at the end of the first interpolation, which are used in the second interpolation of energy at the grid G.

$$\Delta F_x=\Delta F\cos(\theta_k)$$
$$\Delta F_y=\Delta F\sin(\theta_k)$$

where θ_k is the angle between the wave direction and the x-axis. The new position attained by the wave packets is

$$\begin{aligned} x&=\tilde{x}+\Delta F_x \\ y&=\tilde{y}+\Delta F_y \end{aligned} \qquad (2)$$

where $(\tilde{x}, \tilde{y})$ is the original position of the grid.

For interpolating the energy to the grid point, a two-step interpolation method is used. In the first interpolation step, the wave energies are obtained at points on the lines of fixed x, through interpolating the wave energies of the two nearby wave packet. In the second step of the interpolation, the energies on these lines are used for obtaining the energy at the exact grid point.

In detail, in the first interpolation, the wave energies at the new positions attained by the wave packets started from the grid and from a grid nearby to that grid are used. The selection of the nearby grids depends only on the value

of θ_k at the grid. A schematic diagram for the explanation of these procedures is shown in Fig. 7, for the case of $0°<\theta_k<90°$. If θ_k is $-90°>\theta_k\geq 90°$, (i, j) and the $(i, j-1)$ grids are selected for the first interpolation and for the other values of θ_k, $(i, j+1)$ is selected. The wave energy is treated here as a vector quantity with its magnitude of energy value and the direction of propagation. After this grid selection, the energy at the crossing point (C or C′) of a line formed by joining the new energy positions (A and B or A′ and B′) is vector interpolated.

After finishing this first interpolation for all grids, the wave energy available at the newly fixed points (C and C′) are used in the second interpolation to get the energy exactly present at the grid points. Two such crossing points are so selected that both of them have the same x co-ordinate as that of the particular grid for which the interpolation is going on, but as to the y co-ordinate, one must be greater and of the other one must be lesser than that of the selected grid. Two such points nearest to the grid are fixed and the energy at the original grid is interpolated from the energy at the above mentioned points. Hence, the present interpolation at a particular grid uses the energy corresponding to three nearby grids and of the self.

References

BRETSCHNEIDER, C. L. (1968): Decay of wind generated waves to ocean swell by significant wave method, Fundamentals of ocean engineering—Part 8. Ocean Industry, March, 36-39, 51.

BRETSCHNEIDER, C. L., H. L. CRUTCHER, J. DARBYSHIRE, G. NEUMANN, W. J. PIERSON, H. WALDEN and B. W. WILSON (1962): Data for high wave conditions observed by the OWS "Weather Reporter" in December 1959. Duetsch. Hydrogr. Zeit., **15**, 243-255.

GÜNTHER, H., W. ROSENTHAL, T. J. WEARE, B.A. WORTHINGTON, K. HASSELMANN and J. W. EWING (1979): A hybrid parametrical wave prediction model. J. Phys. Oceanogr., **84**, 5727-5738.

HASSELMANN, K., T. P. BARNETT, E. BOUWS, H. CARLSON, E. D. CARTWRIGHT, K. ENKE, J. A. EWING, H. GIENAPP, D. E. HASSELMANN, P. KRUSEMAN, A. MEERBURG, P. MÜLLER, D. J. OLBERS, K. RICHTER, W. SELL and H. WALDEN (1973): Measurements of wind-wave growth and swell decay during the Joint North Sea Wave Project (JONSWAP), Deutsch. Hydrogr. Z., Suppl. A., **8(12)**.

HASSELMANN, K., D. B. ROSS, P. MÜLLER and W. SELL (1976): A parametrical wave prediction model. J. Phys. Oceanogr., **6**, 201-228.

HATORI, M., M. TOKUDA and Y. TOBA (MS.): On the strong interaction between regular waves and wind waves (submitted to J. Oceanogr. Soc. Japan).

ISOZAKI, I. (1978): Recent progress in ocean wave prediction and some problems for its further advances. Umi to Sora, **53**, 47-60 (in Japanese).

ISOZAKI, I. and T. UJI (1973): Numerical prediction of ocean wind waves. Pap. Met. Geophys., **24**, 207-231.

KAWAI, S., P. S. JOSEPH and Y. TOBA (1979): Prediction of ocean waves based on the single-parameter growth equation of wind waves. J. Oceanogr. Soc. Japan, **35**, 151-167.

LONGUET-HIGGINS, M. S. (1952): On the statistical distribution of the heights of the sea waves. J. Mar. Res., **11**, 245-266.

MITSUYASU, H., F. TASAI, T. SUHARA, S. MIZUNO, M. OHKUSA, T. HONDA and K. RIKIISHI (1980): Observation of the power spectrum of ocean waves using a cloverleaf buoy. J. Phys. Oceanogr., **10**, 286-296.

TOBA, Y. (1972): Local balance in the air-sea boundary processes, I. On the growth process of wind waves. J. Oceanogr. Soc. Japan, **28**, 109-120.

TOBA, Y. (1973): Local balance in the air-sea boundary processes, III. On the spectrum of wind waves. J. Oceanogr. Soc. Japan, **20**, 221-226.

TOBA, Y. (1978): Stochastic form of the growth of the wind waves in a single-parameter representation with physical interpretation. J. Phys. Oceanogr., **8**, 469-507.

WILSON, B. W. (1965): Numerical prediction of ocean waves in the North Atlantic for December 1959. Deut. Hydrogr. Zeit., **18**, 114-130.

風波の単一パラメータ発達方程式に基づく海洋波浪の予測 (II) 格子点法の導入

Paimpillil S. JOSEPH*, 河合三四郎*, 鳥羽良明*

要旨: TOBA (1978) の風波の単一パラメータ発達方程式に基づくこの題目の第1報 (KAWAI *et al.*, 1979) の海洋波浪予測モデルの改良を行なった．前報で述べた問題点，すなわち，空間の固定点における時系列予測値が得られないことがあること，および，エネルギーの空間的なかたよりを生じる可能性があることの2点を格子点法の導入によって解決した．改良したモデルを前報と同じ現実の場に適用し，風波とうねりそれぞれについて波高と周期の事後予測を行ない，観測値との比較を行なった．その結果，いずれの量についても良い一致がみられた．

* 東北大学理学部地球物理学教室
〒980 仙台市荒巻字青葉